Supporting Information

Lomenick et al. 10.1073/pnas.0910040106

SI Text

Mass Spectrometry of DB-Bound, Proteolysis-Resistant Proteins in DARTS. Mass spectrometry analysis of the protected band from Fig. 2*A* reveals significant enrichment (P <1.0E-45) of EF-1α isoforms (EEF1A1, 18.7-fold; EEF1A2, 21.7-fold). Although PGK1 and ENO1 levels were comparable with those of EF-1α, PGK1 enrichment was much lower (2.4-fold; P < 1.0E-45), and ENO1 was slightly depleted (−1.8-fold; P = 1.8E-42). The result could indicate lower-affinity binding of DB to PGK1 or secondary effects on protein abundance because in this experiment the cells were treated with drug in vivo. SUCLA2 (11.7-fold) and BAT1 (7.5-fold) were enriched intermediately (and possibly indirectly as well because of the in vivo treatment), but because they were >100 times less abundant than EF-1α, they could not account for the increase in the protected band intensity.

DARTS Using Different Proteases. The proteome encodes a wide range of susceptibility to proteolysis, and each protein has its own unique resistance signature against a panel of proteases. We found that although thermolysin worked well for DARTS with many target proteins, its weakness lay in the fact that a significant proportion of the proteome is highly resistant to proteolysis by thermolysin, even after allowing the digestion to proceed for several hours or overnight. This is consistent with previously published observations (1) and, in effect, limits the utility of thermolysin as an enzyme for DARTS.

Our effort to overcome the limitations of thermolysin initially led us to try subtilisin. In our hands, subtilisin could be used successfully with DARTS for several target proteins (Fig. 1*B* and Fig. S4*A*). Additionally, subtilisin proved to be much more robust than thermolysin and was able to digest almost all proteins into smaller fragments and peptides at much lower concentrations than thermolysin. However, the magnitude of protection of the target protein achievable with subtilisin appeared to be less than with thermolysin. This could be explained by the ability of subtilisin to proteolyse native, folded proteins, whereas thermolysin requires its substrates to be unfolded. Alternatively, the substrate residues of subtilisin may simply have been more accessible in the structures of the target proteins tested than those of thermolysin, and different results would be seen with other proteins.

As an alternative to using a single protease, we hypothesized that perhaps a mixture of many different enzymes would provide the best overall digestion efficiency and magnitude of target protein protection. To test this, we initially chose to use pronase (Roche), a commercially available protease mixture containing endo- and exoproteases capable of digesting native and unfolded proteins. As seen in Fig. S4*B*, pronase was able to achieve a similar overall level of digestion as subtilisin at various concentrations while permitting a more pronounced protective effect of EF-1A by DB. These results suggest that pronase or other protease mixtures may prove to be most useful for DARTS, given its ability to break down virtually all proteins into individual amino acids at sufficiently high concentrations.

Limitations of Existing Affinity-Based Target Identification Methods. Traditionally, affinity chromatography plays a major role in the identification of the binding targets for many biologically active small molecules and natural products (reviewed in refs. 2 and 3). However, this and other newly developed affinity-based techniques require derivatization of the drug of interest into a form amenable for "pulldown" of target proteins, e.g., by covalently attaching the small molecule onto a solid support or labeling the molecule with an affinity (e.g., biotin) or fluorescent tag, photoreactive group, or radioisotope (4, 5). Many, if not the majority of, drugs have never been successfully derivatized for these purposes, because both of the high likelihood that bioactivity is lost/altered upon modification of the compound and of the enormous investment of time and expertise required to examine the viability of this approach per se (and to do so anew for each different molecule).

In addition to affinity chromatography, many new methods for drug target identification have been developed, ranging from biochemistry to genetics, proteomics, and imaging (3, 4, 6–14). All current target identification methods are of two main categories: affinity-based methods, which detect the direct binding of the drug to its target(s), and phenotype-based methods, which infer drug targets/pathways from the physiological responses or biochemical signatures the drugs produce.

Matrix-based affinity detection fuses the small molecule of interest to a solid support, e.g., Affi-Gel resin beads (15) or glass slides (16) or to a capturable moiety such as biotin (4). Matrix-free affinity labeling relies on the incorporation of radioisotope, photoreactive, or fluorescent labels into the small molecule of interest (4, 5). Therefore, all current affinity methods are limited to small molecules that contain derivatizable functionalities and whose bioactivity/binding is unaffected by the modification. Other barriers in affinity chromatography include molecules (especially natural products) that are difficult or impractical to synthesize. This becomes especially daunting because essentially every small molecule is unique. Although a "tagged" library approach has been adopted to facilitate downstream target identification (16–20), it imposes additional constraints on chemical diversity.

Resveratrol Target Analysis. For cytotoxic and cytostatic small molecules, deletion mutants in their target often would have increased sensitivity to the drug (and overexpression could decrease sensitivity). Indeed, this is the basis for the elegant haploinsufficiency profiling (HIP) strategy (21). However, an inherent limitation of this type of fitness-based methods is that they are applicable only to drugs that affect cell growth/viability, i.e., cytotoxic or cytostatic drugs. Resveratrol, just like most bioactive food compounds, exhibits very low potency and causes no detectable cytotoxicity even at saturating concentrations. In fact, resveratrol added at a final concentration of ≈1 mM precipitated out of the culture medium but did not cause detectable inhibition of yeast growth—not in the wild type, nor in *tif1* or *tif2* deletion mutants (Fig. S7). A key advantage of DARTS is that it is independent of the drug's biological phenotype, and thus is not limited to the studies of cytotoxic/cytostatic drugs or drugs that induce transcriptional or morphological changes which have been the limitation of previous methods.

Materials and Methods. ***Reagents.*** Recombinant human FKBP12 was purchased from R&D Systems (Cat. no. 3777-FK). The recombinant human FRAP1 (mTOR) fragment corresponding to amino acids 1360–2549 (163.9 kDa, ≈70% purity) was obtained from Invitrogen (Cat. no. PV4753). The proteases subtilisin Carlsberg (Cat. no. P5380) and thermolysin (Cat. no. 88303) were purchased from Sigma. Stock solutions of each protease were made, aliquoted, and stored at −20 °C. New aliquots were used for each proteolysis experiment. For Western

blotting, anti-EF1A1 (Cat no. 37969; Abcam), anti-GAPDH (Cat. no. 4300; Ambion), and anti-FLAG (Sigma) antibodies and the streptavidin–horseradish peroxidase conjugate (Streptavidin-HRP) from the Transcend Chemiluminescent Non-Radioactive Translation Detection System (Promega) were used. Coomassie and silver staining were performed by using SimplyBlue and the SilverQuest staining kit from Invitrogen. Protein concentration was measured by using the BCA protein assay kit (Pierce).

Plasmids. The bicistronic translation reporter construct pcDNA/REN/HCV/FF was described previously (22). pcDNA/FF/EMCV/REN was generated by subcloning the XhoI-BamHI fragment from pKS/FF/EMCV/REN (23) into pcDNA3.1(−) using the same restriction sites.

For IVT, pcDNA3.1-hTOR1968C was generated by PCR cloning of mTOR coding region 5902–7650 (corresponding to hTOR amino acids 1968–2549) into pcDNA3.1 using the EcoRI and KpnI sites; the PCR template was a cDNA mixture that was synthesized by reverse transcription of total RNA isolated from HEK293 cells. pcDNA3.1-hTOR1968C/S2035T was generated similarly except using pBJ5-FLAG-FRAP/S2035T (24) as PCR template. pcDNA3.1-FLAG-hTOR was generated by ligating a NotI-KpnI fragment (containing FLAG + mTOR coding region 1–5901) from pBJ5-FLAG-FRAP·S2035T (24) and a KpnI fragment with PCR'd hTOR coding region 5902–7650 into pcDNA3.1 using the NotI and KpnI sites. All constructs were verified by DNA sequencing.

DARTS with pure proteins. For Fig. 1*B*, 40 ng/μL (≈3 μM) recombinant FKBP12 was incubated with rapamycin, FK506, wortmannin (100 μM each), or DMSO solvent control for 2 h at 4 °C, followed by digestion with subtilisin at room temperature. Proteolysis 1, 1:100 (wt:wt) subtilisin:FKBP12 for 3 h; Proteolysis 2, 1:10 (wt:wt) subtilisin:FKBP12 for 30 min. For Fig. 1*C*, 200 ng of recombinant FRAP1 (mTOR) was incubated with E4 or DMSO solvent control for 30 min at 4 °C, followed by digestion with 20 ng of thermolysin for 1 h at room temperature.

Sample preparation for mass spectrometry. Bands from 1D SDS/PAGE gels were cut out and prepared for mass spec analysis as described previously (25, 26). Briefly, each band was destained by washing twice in 200 μL of 50 mM NH_4HCO_3, 50% acetonitrile for 15 min with slow vortexing, followed by dehydrating with 100 μL of 100% acetonitrile and drying by speedvac. Reduction was performed with 30 μL of 10 mM DTT, 10 mM TCEP for 30 min at 56 °C. The bands were then washed with 100 μL of 50 mM NH_4HCO_3, 50% acetonitrile and dehydrated with 100 μL of 100% acetonitrile. Alkylation was performed with 100 μL of 100 mM iodoacetamide for 30 min in the dark, followed by washing twice in 200 μL of 50 mM NH_4HCO_3, 50% acetonitrile for 2 min with slow vortexing. The bands were then dehydrated with 200 μL of 100% acetonitrile and dried by speedvac.

Each band was rehydrated in 30 μL of 50 mM NH_4HCO_3 (pH 8.0) containing 20 ng/μL of trypsin on ice for 15 min. Remaining trypsin solution was replaced with 30 μL of 50 mM NH_4HCO_3 (pH 8.0). In-gel tryptic digestion was then performed overnight at 37 °C. Digestion was halted with 5 μL of 5% aqueous TFA. Peptides were extracted by shaking the solution for 15 min, saving the solution, and replacing with 30 μL of 50% acetonitrile and 0.1% TFA and shaking for 15 min twice. The extracted peptides were then concentrated to 25 μL by speedvac.

Mass spectrometry. Tryptic peptides were analyzed by LC/MS/MS on a Thermo LTQ-Orbitrap mass spectrometer with an Eksigent LC pump. The peptides were loaded onto a C18 reverse-phase column at a flow rate of 3 μL/min. Mobile phase A was 0.1% formic acid and 2% ACN in water; mobile phase B was 0.1% formic acid and 20% water in ACN. Peptides were eluted from the column at a flow rate of 220 nL/min by using a linear gradient from 5% B to 50% B over 60 min, then to 95% B over 5 min, and finally keeping constant 95% B for 5 min. Spectra were acquired in data-dependent mode (using dynamic exclusion of 30 sec for fragmented peptides) with the Orbi-trap used for MS scans and LTQ for MS/MS scans.

Proteins were initially identified by searching the spectra against the human International Protein Index database (version 3.46) and the *S. cerevisiae* Swissprot database (May 2008) using the SEQUEST algorithm (27) integrated into the Bioworks software package. Each peptide met the following criteria: XCorr ≥ 2(+1), ≥ 3(+2), ≥ 4(+3), ≥ 5(+4), and DeltaCN >0.1. For quantitative comparison of protein and peptide abundances, MS spectra were analyzed by using the differential workflow of the Rosetta Elucidator software system (Rosetta Inpharmatics) (28). Annotation was performed by using PeptideTeller and ProteinTeller with a minimum probability of 0.99 and predicted error of 0.0. Protein ratio data were generated with a *P* value cutoff of 0.01 for all proteins with a peptide number >1. Intensity scaling was performed against the mean of feature signals, with 10% of outliers removed from the baseline dataset. Similar results were obtained in analysis without intensity scaling (Fig. S6*A*). Analysis of a control band from the same gel in the Didemnin B experiment that stained at the same intensity in both lanes revealed no significant differences in protein levels (Fig. S6*B*).

In vivo translation assays. HEK293 cells in DMEM + 10% FBS were pretreated with 50 μM resveratrol for 1 h and transfected with bicistronic translation reporter plasmids using LipoD293 DNA in vitro transfection reagent (SignaGen). Two hours after transfection, cells were washed with PBS, seeded in 96-well format, and treated with resveratrol or vehicle control. Reporter activity was measured 33 h after transfection by using the Dual-Glo luciferase assay system (Promega) with an Analyst HT plate reader (Molecular Devices).

We analyzed the effect of resveratrol on different luciferase assay systems using in vitro translated firefly luciferase, and found that the effect of resveratrol on firefly luciferase reaction is kit dependent. For example, in the Bright-Glo kit (Cat. no. E2610; Promega), firefly luciferase readout is significantly decreased in the presence of resveratrol, as shown by ref. 29. On the contrary, in the Dual-Glo kit (Cat. no. E2940; Promega), resveratrol has little or no inhibition on firefly luciferase readout. Our data in Fig. 3*D* were based on the Dual-Glo kit, in which the luciferase reaction is not affected by resveratrol. Also, there was no resveratrol added to the in vitro luciferase assay reactions in Fig. 3*D*. Rather, resveratrol was used to treat cells and washed away before the cells were lysed for luciferase assay.

C. elegans lifespan analysis. N2 wild-type strains were maintained at 20 °C on standard nematode growth medium (NGM) seeded with *Escherichia coli* OP50 as described (30). *E. coli* RNAi strains were obtained from Open Biosystems; clones were verified by sequencing. To make NGM plates containing resveratrol or vehicle, 240 μL of a solution containing 2.5 mM resveratrol (or the equivalent amount of ethanol, for vehicle control), 20% DMSO, 20% ethanol, 10% PBS, and 50% ddH20 were spread on top of the NGM plate, making a 50 μM final concentration of resveratrol in the plate. Resveratrol was dissolved in 95% ethanol and stored at 4 °C.

Lifespan analysis was conducted with N2 worms at 20 °C. Eggs were added to NGM plates containing OP50. At the L4 stage, worms were washed off and placed onto bacterialess NGM plates for 60 min so that the worms can digest the remaining OP50 in their gut. Then worms were moved onto NGM plates containing *gfp*, *daf-16*, or *inf-1* RNAi with resveratrol or vehicle. Ampicillin (50 μg/mL) and isopropyl β-D-thiogalactopyranoside (IPTG) (1 mM) were used to select for the RNAi *E. coli* and to induce the expression of dsRNA, respectively. Initially, 100 worms were picked for each treatment. During their egg-laying days, the worms were transferred to new plates every day, and then every

other fourth day thereafter. To assess the survival of the worms, the animals were prodded with a platinum wire every other day, and those that failed to respond were scored as dead. Worms that died as a result of bagging or vulva bursting, as well as those that crawled off the plate, were not included in the study.

DARTS using cell lysates incubated in vitro with didemnin B. For Fig. S2, human Jurkat cells were lysed in M-PER (Pierce) supplemented with protease and phosphatase inhibitors. Protein concentration was determined by BCA Protein Assay kit (Pierce). Lysates were incubated with DMSO control, or DB from 1 ng/mL to 1 μg/mL, for 30 min at room temperature. Samples were then divided into two aliquots, each of which underwent proteolysis with thermolysin or mock proteolysis, respectively, followed by Western blot analysis.

DARTS using yeast cell lysates. For Fig. S3*C*, yeast cells expressing a His-tagged F-box protein were cultured to mid-log phase (1.0×10^7 cells per milliliter) and treated with the SCF ubiquitin E3 ligase inhibitor at indicated concentrations for 45 min. Then cells were pelleted, washed once with water, and lysed in Triton-lysis buffer with FastPrep. Protein concentration of the lysate was measured by using BCA Protein Assay kit (Pierce). For DARTS, 54 μg of lysate was used in 10 μL (total) reaction. For proteolysis, 20 ng of thermolysin was used for one reaction.

For the DARTS experiment using yeast cell lysates incubated in vitro with resveratrol, BY4742 cells were suspended in yeast extraction buffer (31) [(40 mM Hepes/KOH (pH 7.5), 350 mM NaCl, 0.5 mM DTT, 10% glycerol, 0.1% Tween-20) supplemented with Roche complete protease inhibitor mixture (Roche Diagnostics)]. Cell pellets were broken with glass beads for 2×40 s at 4 °C in a FastPrep-24 (MP Biomedicals). Whole-cell lysates were collected after centrifugation (1,500 rpm using Beckman Coulter Microfuge 22R with F241.5P rotor, 10 min). Lysates were incubated with ethanol control or 1 mM resveratrol for 30 min at room temperature. Samples were then divided into two aliquots that underwent proteolysis with thermolysin or mock proteolysis.

1. Park C, Zhou S, Gilmore J, Marqusee S (2007) Energetics-based protein profiling on a proteomic scale: Identification of proteins resistant to proteolysis. *J Mol Biol* 368:1426–1437.
2. Katayama H, Oda Y (2007) Chemical proteomics for drug discovery based on compound-immobilized affinity chromatography. *J Chromatogr B* 855:21–27.
3. Terstappen GC, Schlupen C, Raggiaschi R, Gaviraghi G (2007) Target deconvolution strategies in drug discovery. *Nat Rev Drug Discov* 6:891–903.
4. Sleno L, Emili A (2008) Proteomic methods for drug target discovery. *Curr Opin Chem Biol* 12:46–54.
5. MacKinnon AL, Garrison JL, Hegde RS, Taunton J (2007) Photo-leucine incorporation reveals the target of a cyclodepsipeptide inhibitor of cotranslational translocation. *J Am Chem Soc* 129:14560–14561.
6. Tochtrop GP, King RW (2004) Target identification strategies in chemical genetics. *Comb Chem High Throughput Screen* 7:677–688.
7. Walsh DP, Chang YT (2006) Chemical genetics. *Chem Rev* 106:2476–2530.
8. Bharucha N, Kumar A (2007) Yeast genomics and drug target identification. *Comb Chem High Throughput Screen* 10:618–634.
9. Perrimon N, Friedman A, Mathey-Prevot B, Eggert US (2007) Drug-target identification in *Drosophila* cells: Combining high-throughout RNAi and small-molecule screens. *Drug Discov Today* 12:28–33.
10. Huang J, et al. (2004) Finding new components of the target of rapamycin (TOR) signaling network through chemical genetics and proteome chips. *Proc Natl Acad Sci USA* 101:16594–16599.
11. Perlman ZE, et al. (2004) Multidimensional drug profiling by automated microscopy. *Science* 306:1194–1198.
12. Eggert US, et al. (2004) Parallel chemical genetic and genome-wide RNAi screens identify cytokinesis inhibitors and targets. *PLoS Biol* 2:e379.
13. Young DW, et al. (2008) Integrating high-content screening and ligand-target prediction to identify mechanism of action. *Nat Chem Biol* 4:59–68.
14. Cravatt BF, Wright AT, Kozarich JW (2008) Activity-based protein profiling: from enzyme chemistry to proteomic chemistry. *Annu Rev Biochem* 77:383–414.
15. Wan Y, et al. (2004) Synthesis and target identification of hymenialdisine analogs. *Chem Biol* 11:247–259.
16. MacBeath G, Koehler AN, Schreiber SL (1999) Printing small molecules as microarrays and detecting protein-ligand interactions en masse. *J Am Chem Soc* 121:7967–7968.
17. Mitsopoulos G, Walsh DP, Chang YT (2004) Tagged library approach to chemical genomics and proteomics. *Curr Opin Chem Biol* 8:26–32.
18. Hergenrother PJ, Depew KM, Schreiber SL (2000) Small-molecule microarrays: Covalent attachment and screening of alcohol-containing small molecules on glass slides. *J Am Chem Soc* 122:7849–7850.
19. Barnes-Seeman D, Park SB, Koehler AN, Schreiber SL (2003) Expanding the functional group compatibility of small-molecule microarrays: Discovery of novel calmodulin ligands. *Angew Chem Int Ed Engl* 42:2376–2379.
20. Bradner JE, et al. (2006) A robust small-molecule microarray platform for screening cell lysates. *Chem Biol* 13:493–504.
21. Giaever G, et al. (1999) Genomic profiling of drug sensitivities via induced haploinsufficiency. *Nat Genet* 21:278–283.
22. Bordeleau ME, et al. (2006) Functional characterization of IRESes by an inhibitor of the RNA helicase eIF4A. *Nat Chem Biol* 2:213–220.
23. Novac O, Guenier AS, Pelletier J (2004) Inhibitors of protein synthesis identified by a high throughput multiplexed translation screen. *Nucleic Acids Res* 32:902–915.
24. Brown EJ, et al. (1995) Control of p70 s6 kinase by kinase activity of FRAP in vivo. *Nature* 377:441–446.
25. Shevchenko A, Wilm M, Vorm O, Mann M (1996) Mass spectrometric sequencing of proteins silver-stained polyacrylamide gels. *Anal Chem* 68:850–858.
26. Edmondson RD, et al. (2002) Protein kinase C epsilon signaling complexes include metabolism- and transcription/translation-related proteins: Complimentary separation techniques with LC/MS/MS. *Mol Cell Proteomics* 1:421–433.
27. Eng JK, Mccormack AL, Yates JR (1994) An approach to correlate tandem mass-spectral data of peptides with amino-acid-sequences in a protein database. *J Am Soc Mass Spectrom* 5:976–989.
28. Neubert H, et al. (2008) Label-free detection of differential protein expression by LC/MALDI mass spectrometry. *J Proteome Res* 7:2270–2279.
29. Bakhtiarova A, et al. (2006) Resveratrol inhibits firefly luciferase. *Biochem Biophys Res Commun* 351:481–484.
30. Brenner S (1974) The genetics of *Caenorhabditis elegans*. *Genetics* 77:71–94.
31. Grant PA, Berger SL, Workman JL (1999) Identification and analysis of native nucleosomal histone acetyltransferase complexes. *Methods Mol Biol* 119:311–317.

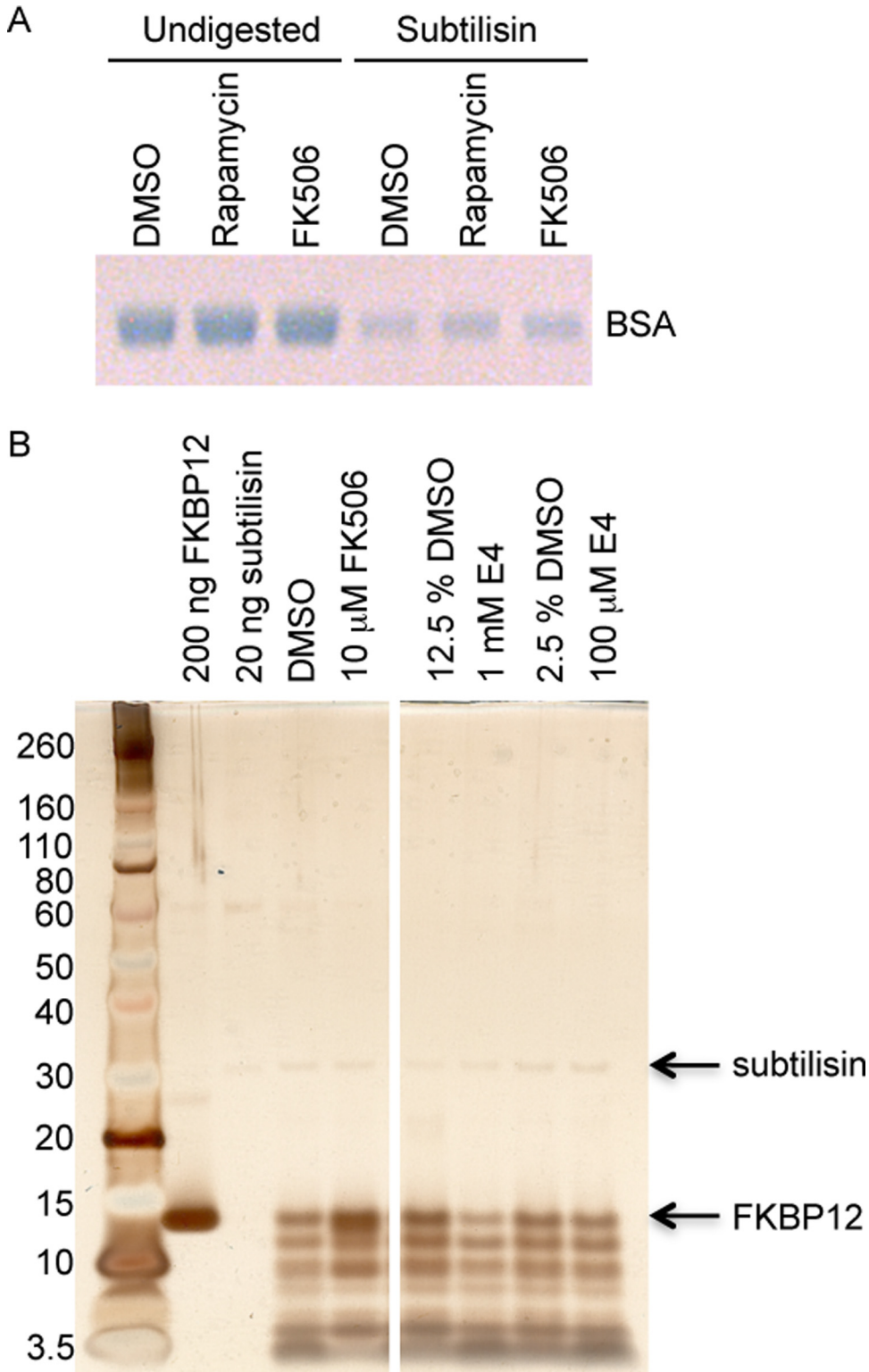

Fig. S1. (*A*) Subtilisin activity is unaffected by the small molecules used for Fig. 1*B* under identical experimental conditions except with BSA as a nonbinder control. (*B*) E4 does not confer proteolysis protection on FKBP12, a control protein that does not bind to the small molecule. C-terminal His_6-tagged human FKBP12 (200 ng) was incubated with E4, FK506 (positive control), or DMSO (solvent control) for 2 h at 4 °C, followed by digestion with 20 ng of subtilisin Carlsberg for 30 min at room temperature. Samples were run on NuPAGE Novex 4–12% Bis-Tris gel (Invitrogen) and silver-stained. Samples above were all run on the same gel.

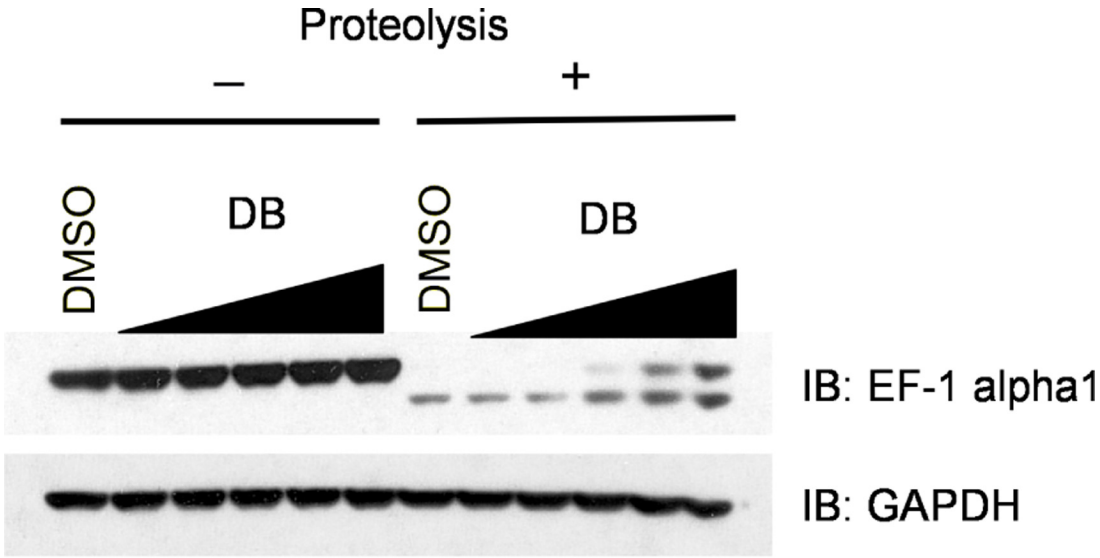

Fig. S2. DARTS with Didemnin B using whole-cell lysates. Lysates from untreated human Jurkat cells were incubated with DMSO control or DB (1 ng/mL, 10 ng/mL, 100 ng/mL, 300 ng/mL, and 1 μg/mL) for 30 min at room temperature. Each sample was then split into two samples that underwent thermolysin proteolysis or mock digestion, respectively, followed by Western blot analysis. Protection can be seen starting at 100 ng/mL.

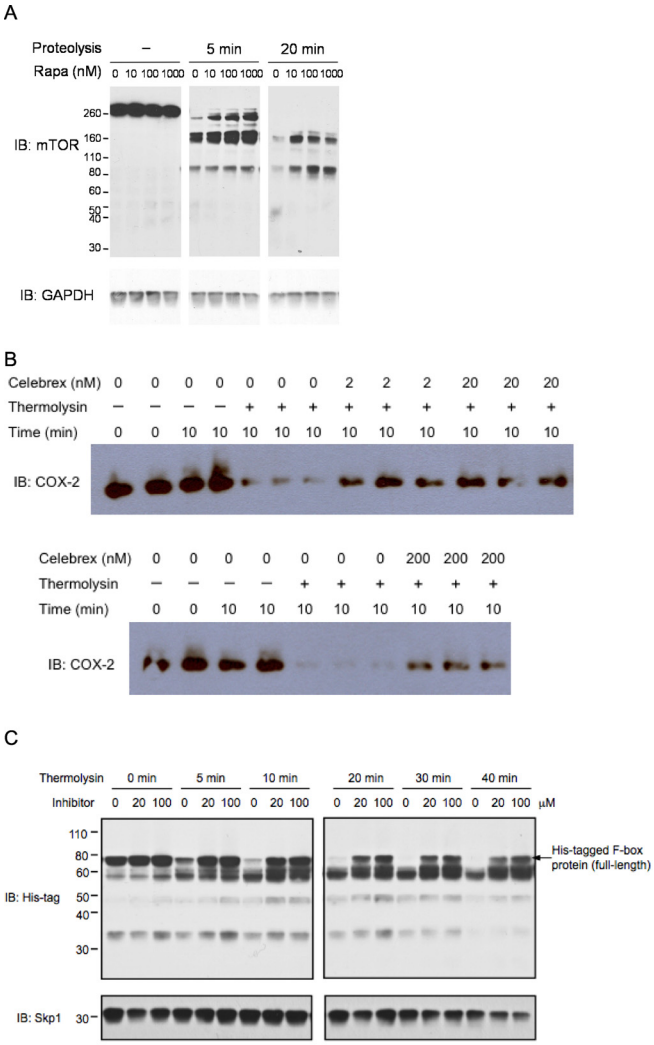

Fig. S3. (*A*) DARTS using rapamycin-treated cells. A549 cells were treated with indicated concentrations of rapamycin, or DMSO control, for 30 min and washed in PBS once before lysis in Triton X-100 lysis buffer [50 mM Tris·HCl (pH 7.5), 0.5% Triton X-100, 200 mM NaCl, 10% glycerol, 1 mM DTT, Roche protease inhibitor mixture, and phosphatase inhibitors (10 mM sodium pyrophosphate, 50 mM NaF, and 0.1 mM orthovanadate)]. Protein concentration was determined by BCA Protein Assay kit (Pierce). Fifty-two microgram of cell lysate was used for DARTS experiment in a total of 10 μL. All steps were performed on ice or at 4 °C to help prevent premature protein degradation. Each sample was then quickly warmed to room temperature and immediately proteolysed with 100 ng of thermolysin for every 52 μg of lysate for the indicated time. To stop the proteolysis reaction, 1 μL of 0.5 M EDTA (pH 8.0) was added to each sample, mixed well, and immediately placed on ice. After adding SDS sample buffer, samples were subjected to 6% Tris·HCl SDS/PAGE and Western blotted with anti-mTOR polyclonal antibody (Cell Signaling Technology). (*B*) DARTS with celecoxib, using cell lysates. Murine RAW264.7 cells were treated with LPS (200 ng/mL) for 18 h, to induce COX2 expression. Cells were washed with cold PBS and lysed with M-PER supplemented with Roche protease inhibitor mixture and phosphatase inhibitors according to manufacturer's instructions (Pierce). Protein concentration was determined by using the Bradford Protein Assay kit (BIO-RAD). Whole-cell lysates were diluted with proteolysis reaction buffer [50 mM Tris·HCl (pH 8.0), 50 mM NaCl, 10 mM $CaCl_2$]. All steps were performed on ice to prevent premature protein degradation. Lysates (24 μg) were incubated with ethyl alcohol vehicle control, or with celecoxib (Panacea Biotec Ltd.) at concentrations of 2, 20, and 200 nM, for 2 h at 9 °C, in triplicate. Untreated lysates diluted to the same final volume were used as controls. Samples were proteolysed with 1 μg of thermolysin (Cat. no. 88303; Sigma) for every 20 μg of lysate at 25 °C for 10 min. To stop the proteolysis the reaction tubes were shifted to 4 °C and EDTA (pH 8.0, 50 mM final concentration) and SDS/PAGE loading buffer were added to each sample. The reaction tubes were then incubated at 100 °C for 10 min. Aliquots of each sample were subjected to electrophoresis on 12% SDS/PAGE. After electrophoresis, proteins were transferred to PVDF membranes. For Western blotting, anti-COX2 antibody sc-1747-R (Santa Cruz Biotechnology) was used. Thermolysin stocks were stored at −20 °C; new thermolysin stocks were used for each proteolysis experiment. The upper and lower illustrations are separate electrophoresis experiments from samples prepared at the same time. Because electrophoresis, transfer, and immunoblotting of the samples treated with 200 nM celecoxib were performed separately from samples treated with 2 and 20 nM celecoxib, untreated extracts and extracts treated with thermolysin in the absence of celecoxib are shown for both gels. (*C*) DARTS using an SCF ubiquitin E3 ligase inhibitor identified from a phenotype-based chemical genetic screen. Yeast cells expressing RGS6H-tagged F-box protein were cultured to midlog phase (1.0×10^7 cells per milliliter) and treated with the inhibitor at indicated concentrations for 45 min. Then cells were pelleted, washed once with water, and lysed in Triton-lysis buffer with FastPrep. Protein concentration of the lysate was measured by using BCA Protein Assay kit (Pierce). For DARTS, 54 μg of lysate was used in a 10-μL (total) reaction. For proteolysis, 20 ng of thermolysin was used for one reaction. The E3 inhibitor protects the F-box protein, but not an associated Skp1 protein, from protease digestion.

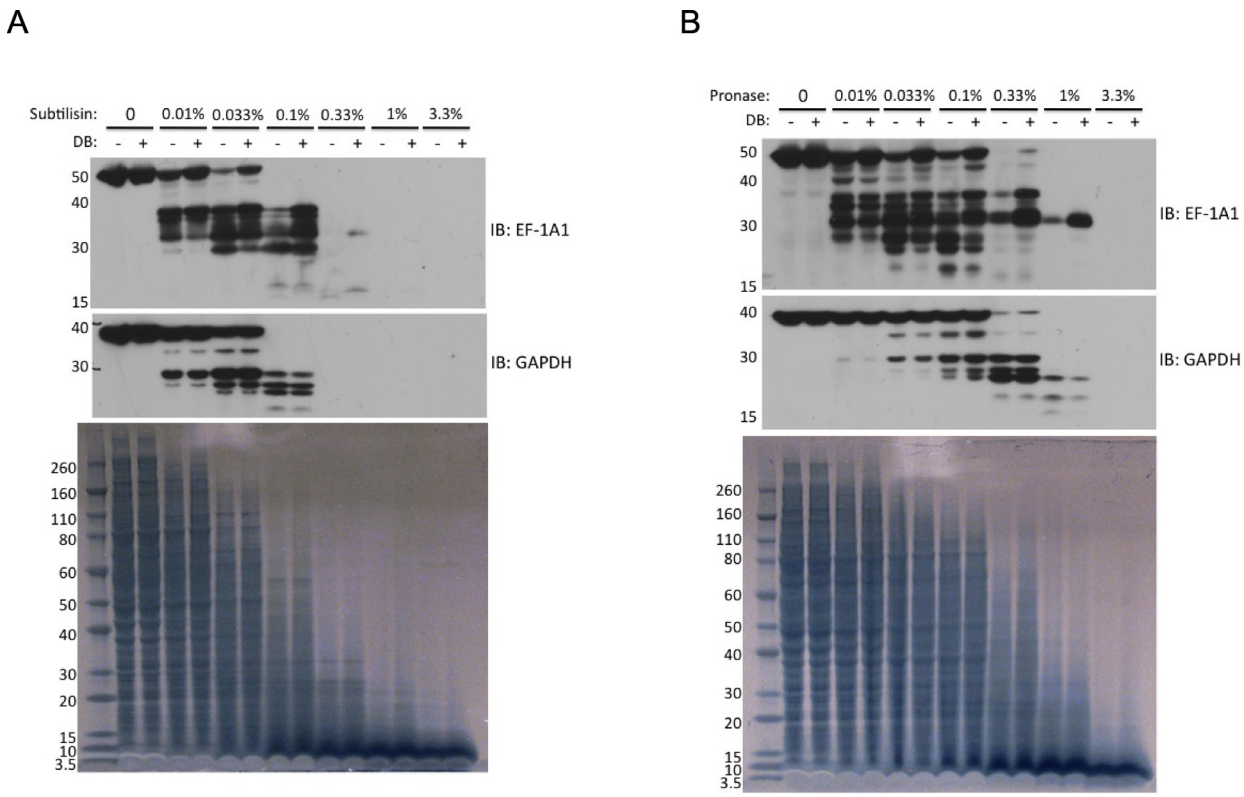

Fig. S4. (*A*) DARTS using subtilisin. Lysates from untreated human Jurkat cells were incubated with DMSO control or DB (1 μg/mL) for 1 h at room temperature. Each sample was then split into seven aliquots that underwent digestion with various concentrations of subtilisin, relative to the total amount of protein per sample, for 30 min at room temperature. Digestion was stopped by adding 5× sample loading buffer and boiling immediately. Half of each sample was then loaded onto one of two 4–12% SDS/PAGE gels for SimplyBlue staining and Western blotting. (*B*) DARTS using pronase. Lysates from untreated human Jurkat cells were incubated with DMSO control or DB (1 μg/mL) for 1 h at room temperature. Each sample was then split into seven aliquots that underwent digestion with various concentrations of pronase, relative to the total amount of protein per sample, for 30 min at room temperature. Digestion was stopped by adding 5× sample loading buffer and boiling immediately. Half of each sample was then loaded onto one of two 4–12% SDS/PAGE gels for SimplyBlue staining and Western blotting.

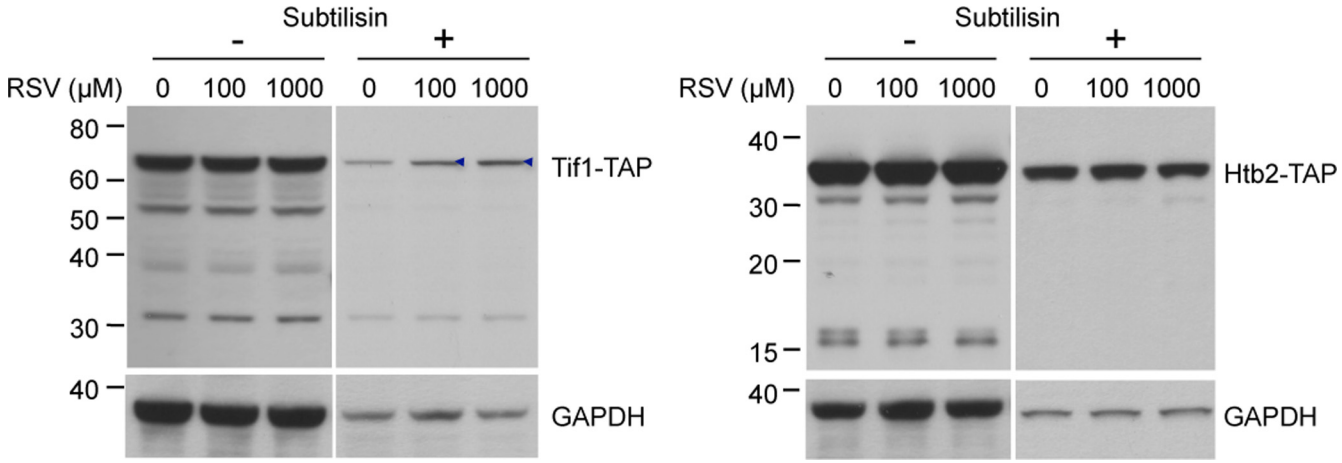

Fig. S5. Resveratrol protects the TAP-tagged Tif1, but not an unrelated control Htb2, from proteolysis. Purple arrow, protein protected from proteolysis.

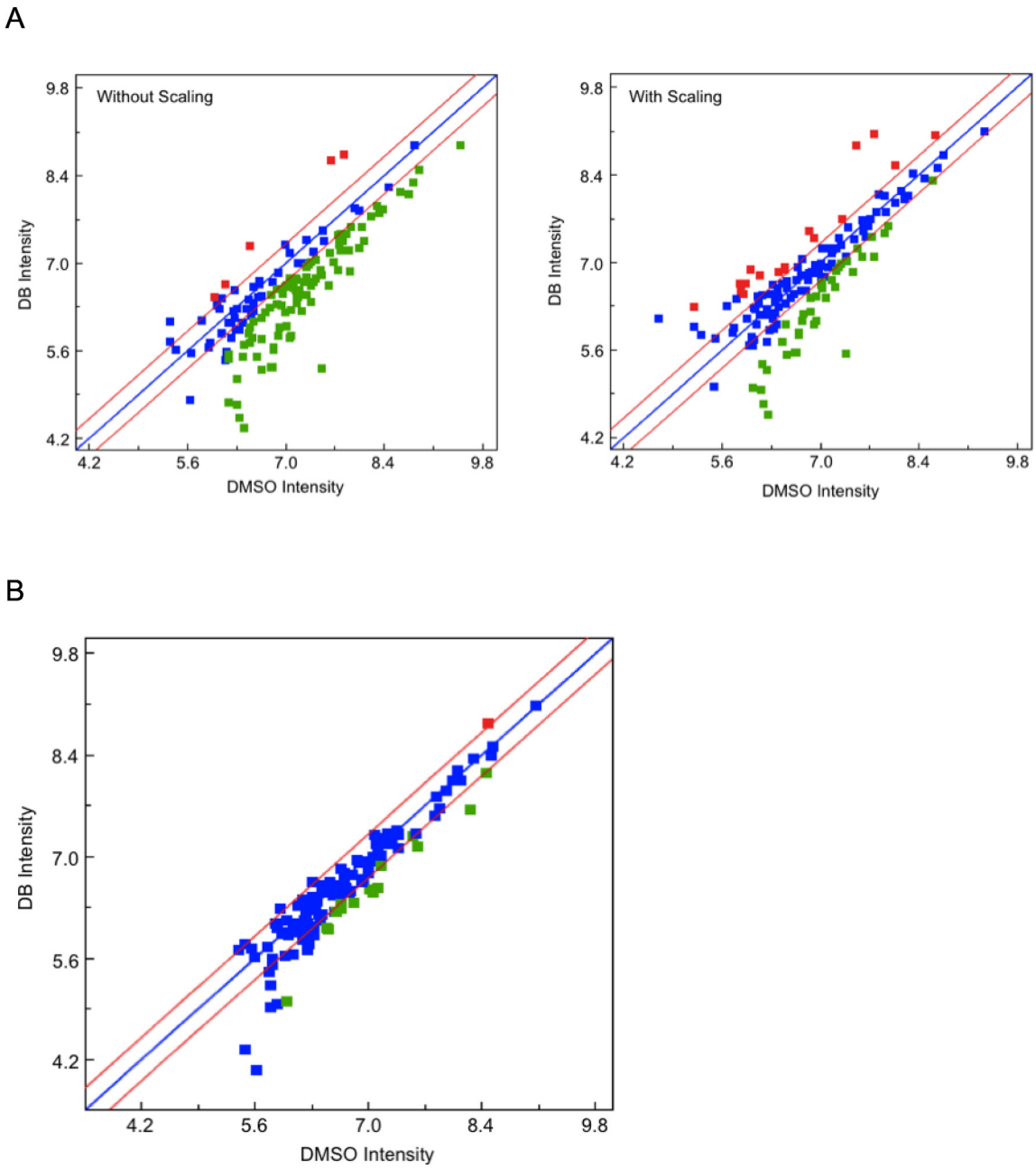

Fig. S6. (*A*) Comparison of MS data analysis with and without intensity scaling. Protein abundance levels for the protected band from Fig. 2*A* were compared by using Rosetta Elucidator both with and without intensity scaling. *x* axis, $\log_{10}$ protein intensity of the DMSO sample; *y* axis, $\log_{10}$ protein intensity of the DB sample. Red dot, protein enriched >2-fold with a *P* value <0.001; green dot, protein depleted >2-fold with a *P* value <0.001; blue dot, unchanged protein. Blue line, ratio = 1; red line, ratio = 2. (*B*) MS analysis of a control band. Protein abundance levels were compared for a control band at 35 kDa with no difference in staining intensity between the DB and control samples after proteolysis. Axes and dots are labeled same as in *A*.

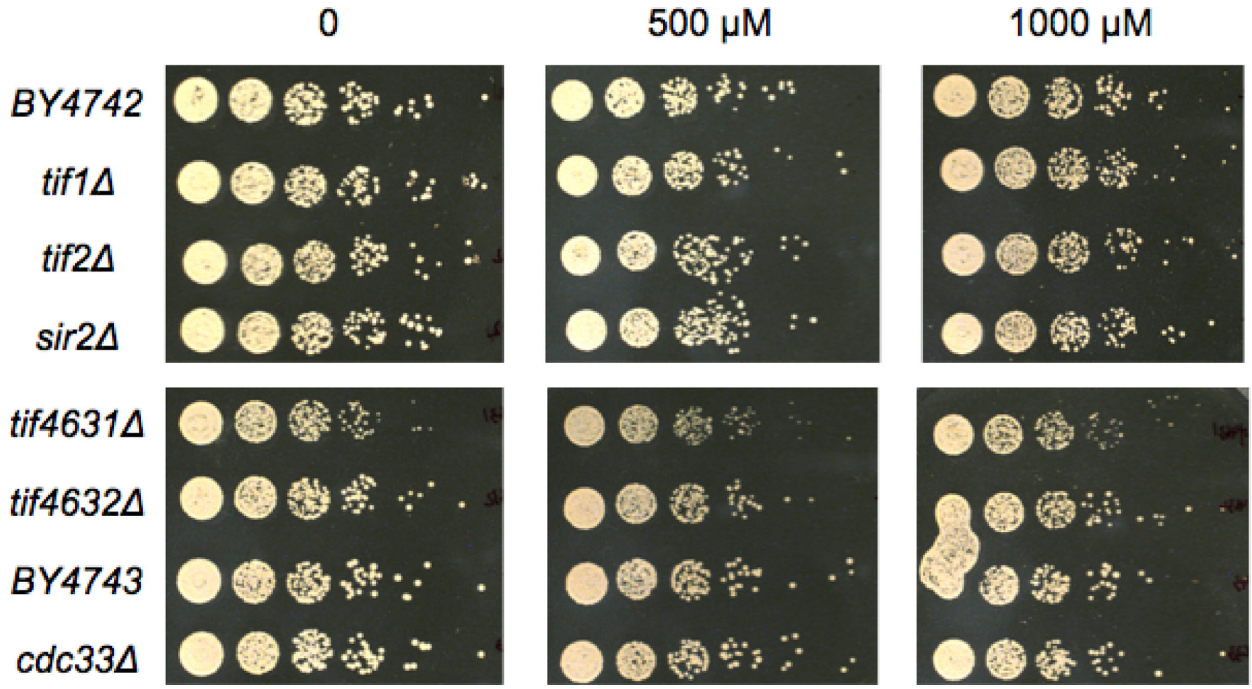

Fig. S7. Resveratrol shows no detectable inhibition of yeast cell growth.

Table S1. Enriched proteins in the resveratrol DARTS sample

Protein	Fold change	*P*	Accession no.	Band
60S ribosomal protein L26-B	11.107	1.35E-04	P53221	Lower
60S ribosomal protein L26-A	9.181	8.12E-27	P05743	Lower
60S ribosomal protein L24	6.05	1.24E-07	P04449, P24000	Upper
40S ribosomal protein S23	4.84	1.05E-04	P32827	Upper
40S ribosomal protein S26	4.701	0.002	P39938, P39939	Upper
60S ribosomal protein L35	3.774	7.27E-18	P39741	Lower
40S ribosomal protein S15	3.677	5.53E-06	Q01855	Lower
60S ribosomal protein L25	3.564	3.45E-21	P04456	Lower
Histone H2A	3.002	3.19E-04	P04911, P04912	Lower
40S ribosomal protein S16	2.906	2.17E-19	P40213	Lower
60S ribosomal protein L21-A	2.777	0.007	Q02753	Upper
60S ribosomal protein L25	2.713	9.60E-05	P04456	Upper
60S ribosomal protein L27-A	2.554	2.37E-04	P0C2H6, P0C2H7	Upper
Ornithine aminotransferase	2.531	9.05E-04	P07991	Lower
40S ribosomal protein S26-B	2.429	4.32E-10	P39938, P39939	Lower
40S ribosomal protein S18	2.412	7.16E-06	P35271	Lower
60S ribosomal protein L34	2.383	1.89E-06	P40525, P87262	Lower
Histone H2B	2.229	5.42E-04	P02293, P02294	Lower
40S ribosomal protein S12	2.07	5.42E-04	P48589	Lower
40S ribosomal protein S19	1.965	3.62E-08	P07280, P07281	Lower
ATP-dependent RNA helicase eIF4A	1.961	0.007	P10081	Upper
60S ribosomal protein L28	1.804	1.72E-04	P02406	Upper
60S ribosomal protein L14-A	1.614	5.05E-04	P36105	Lower
40S ribosomal protein S24	1.481	0.007	P26782	Lower

Other Supporting Information Files

Data Set 1